Effect of the Ligand Structure on the Efficiency of Electron Injection from Excited Ru–Phenanthroline Complexes to Nanocrystalline TiO$_2$ Films

Kohjiro Hara,[†] Hiroaki Horiuchi,[†] Ryuzi Katoh,*,[†] Lok Pratap Singh,[†] Hideki Sugihara,[†] Kazuhiro Sayama,[†] Shigeo Murata,[†] M. Tachiya,[‡] and Hironori Arakawa*,[†]

Photoreaction Control Research Center, National Institute of Advanced Industrial Science and Technology (AIST), 1-1-1 Higashi, Tsukuba, Ibaraki 305-8565, Japan

Received: August 7, 2001; In Final Form: October 31, 2001

We previously reported that the number of anchoring carboxyl groups affects the solar cell performance of dye-sensitized nanocrystalline TiO$_2$ solar cells using Ru–phenanthroline complexes as the sensitizer. To understand the mechanism in detail, the electron injection efficiency of sensitizing dyes adsorbed on nanocrystalline TiO$_2$ films has been studied by transient absorption spectroscopy. We found that the efficiency of electron injection is strongly affected by the number of carboxyl groups of the sensitizing dye, i.e., the efficiency of *cis*-bis(4,7-dicarboxy-1,10-phenanthroline)dithiocyanato ruthenium(II) (with four carboxyl groups) adsorbed on nanocrystalline TiO$_2$ films (DCP2/TiO$_2$) being 4 times as large as that of *cis*-(4-monocarboxy-1,10-phenanthroline)(1,10-phenanthroline)dithiocyanato ruthenium(II) (with one carboxyl group) adsorbed on the same films (MCPP/TiO$_2$). From the analysis of the time profile of the transient absorption, we conclude that the low efficiency of MCPP/TiO$_2$ is due to the presence of inactive dyes on the TiO$_2$ surface, which are not effective for electron injection. By comparing the absorbed photon-to-current conversion efficiencies (APCE) of the solar cells using these films, the effect of the number of the carboxyl groups on the solar cell performance can be attributed to the effect on the injection efficiency of electrons. We have also studied the effect of substitution of the countercations of DCP2. Two protons of carboxyl groups were substituted by two tetrabutylammonium (TBA) ions. The APCE of the DCP2-TBA is higher than that of DCP2, although the relative efficiencies of electron injection are similar for DCP2-TBA and DCP2. This indicates that the rate of reaction of the conducting electrons in the TiO$_2$ film with the I$^-$/I$_3^-$ redox mediators (dark current) is reduced by substituting the protons by TBA ions.

Introduction

A dye-sensitized solar cell (Grätzel cell) consisting of the N3 dye *cis*-bis(4,4′-dicarboxy-2,2′-bipyridine)dithiocyanato ruthenium(II) [Ru(dcbpy)$_2$(NCS)$_2$] adsorbed on nanocrystalline TiO$_2$ films and an I$^-$/I$_3^-$ redox mediator has attracted much attention because of its high solar-energy-to-electricity conversion efficiencies (up to 10% under AM 1.5 irradiation).[1] Many new sensitizer molecules have been synthesized, and the solar cell performance has been evaluated.[2-20] We have also developed new solar cells using newly synthesized Ru complexes,[10-15] Pt complexes[16] and organic dyes.[17-20] Understanding the relation between the solar cell performance and the properties of sensitizer molecules is one of the most important tasks for developing a high performance solar cell. Many molecular properties, such as the redox potential, the light harvesting efficiency, and the lifetime of the excited state, actually correlate with the solar cell performance.

The molecular structure of the sensitizing dye is also an important factor, and therefore, we are studying the effect of the molecular structure on the solar cell performance. Recently, we reported the effect of the number of anchoring carboxyl groups on the solar cell performance of Ru–phenanthroline complexes using *cis*-bis(4,7-dicarboxy-1,10-phenanthroline)-

dithiocyanato ruthenium(II) complex (Ru(dcphen)$_2$ (NCS)$_2$, DCP2) and *cis*-(4-monocarboxy- 1,10-phenanthroline)(1,10-phenanthroline)dithiocyanato ruthenium(II) complex (Ru(mcphen)-(phen)(NCS)$_2$, MCPP) as sensitizing dyes.[14,15] The structures of these dyes are shown in Figure 1. The performance of the solar cell consisting of MCPP (with only one carboxyl group) and the TiO$_2$ film was lower than that of the cell using DCPP (with four carboxyl groups). This clearly shows that the solar cell performance is strongly affected by the small differences in the molecular structure of the sensitizing dye. The counter-cations attached to carboxyl groups also affect the solar cell performance. In fact, when a proton attached to a carboxyl group of DCP2 is substituted by a tetrabutylammonium (DCP2-TBA) cation, the solar cell performance is improved.[13] This again shows that the change in the molecular structure is very important.

Figure 1 shows the primary steps of electron injection and the decay processes of electrons, i.e., the recombination and the reaction with the redox mediator. Upon photoexcitation of the sensitizing dye, the LUMO level of the sensitizing dye is populated. Subsequently, the electron is injected from the LUMO level to the conduction band (CB) of the TiO$_2$ film (electron injection; process 1). The injected electron decays to the HOMO level (recombination; process 2). The oxidized dye can be reduced by the redox mediator (I$^-$/I$_3^-$; rereduction; process 3). The injected electron can also react with the redox

* To whom correspondence should be addressed. E-mail: r-katoh@aist.go.jp and h.arakawa@aist.go.jp.
† Photoreaction Control Research Center, AIST.
‡ AIST.

Nanocrystalline TiO$_2$ Films

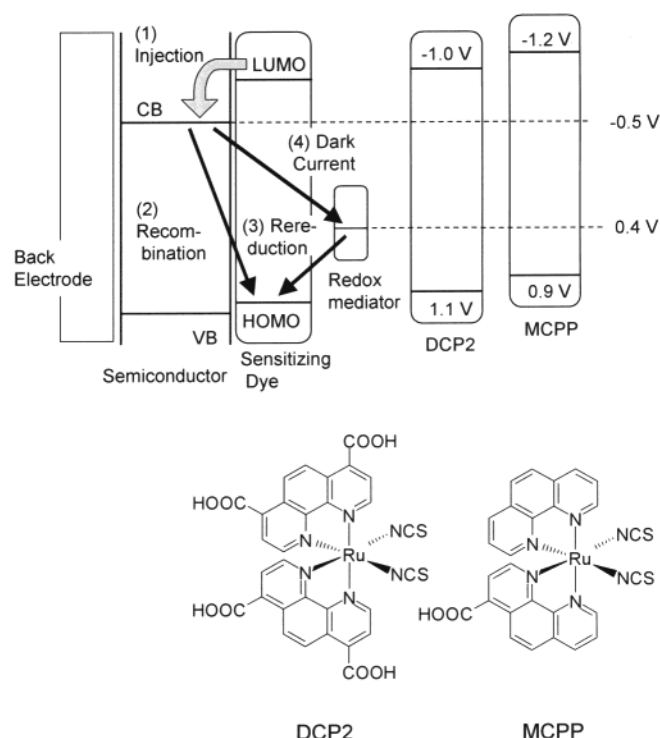*J. Phys. Chem. B, Vol. 106, No. 2, 2002* **375**

Figure 1. Energy level diagram and pathways of the reactions of electrons. Molecular structures of the sensitizers studied are also shown.

mediator during the transport to the back contact electrode (dark current; process 4).

The electron injection (process 1) competes with the relaxation of the excited state of the sensitizing dye. Thus, for electron injection to occur efficiently, it has to be much faster than the unimolecular decay of the excited state of the sensitizing dye. In fact, the rate of electron injection has been extensively studied through femtosecond transient absorption spectroscopy.[21−30] For N3/TiO$_2$, very fast electron injection (<10 ps) has been observed by several authors.[21−25] The injection rate is much faster than the rate of luminescence decay of N3 dye (25 ns),[21] and therefore, the injection efficiency is considered to be almost unity. The recombination process (process 2) has also been studied extensively.[22,31−35] Recombination seemingly occurs very slowly on the order of milliseconds. The rereduction process (process 3) of the oxidized dyes by the redox mediator is completed within 100 ns to 1 μs.[33−35] Namely, the rereduction reaction occurs much faster than the charge recombination, suggesting that almost all electrons injected can remain in the semiconductor. The electrons in the film move to the back electrode on the order of seconds.[36] During the transport, some fraction of the electrons are lost by process 4[37] and the remainder flow into the external circuit.

Figure 1 also shows the energy levels of MCPP, DCP2, TiO$_2$, and the redox mediator studied. The HOMO and LUMO levels of DCP2 are 1.1 and −1.0 V vs NHE, respectively, and those of MCPP are 0.9 and −1.2 V vs NHE, respectively.[14,15] The conduction band edge of a TiO$_2$ electrode and the level of the I$^-$/I$_3^-$ redox mediator were reported to be −0.5 and 0.4 V vs NHE, respectively.[38,39] The LUMO levels of MCPP and DCP2 are sufficiently higher than the energy level of the conduction band edge of TiO$_2$, and therefore, electron injection is possible. The HOMO levels of these sensitizers are located below the energy level of the redox couple, suggesting rereduction reaction to occur.

We have studied the efficiency of the electron injection in the dried films of DCP2 adsorbed on TiO$_2$ (DCP2/TiO$_2$) and

of MCPP/TiO$_2$ by nanosecond transient absorption spectroscopy and the absorbed photon-to-current conversion efficiency (APCE) of the solar cells consisting of these films. We found that the relative efficiency of electron injection from DCP2 to TiO$_2$ is four times as large as that from MCPP to TiO$_2$. From the time profile of the transient absorption, we concluded that the low efficiency of MCPP/TiO$_2$ is due to the presence of inactive dyes on the TiO$_2$ surface, which are not effective for electron injection. We have also studied the effect of substitution of two protons of the carboxyl groups of DCP2 by tetrabutylammonium (TBA) ions (DCP2-TBA). The APCE of the solar cell using DCP2-TBA is higher than that of DCP2, although the relative injection efficiency of DCP2-TBA/TiO$_2$ is similar to that of DCP2/TiO$_2$. This indicates that the dark current (process 4) is reduced by substituting the protons by TBA ions.

Experimental Section

Preparation of the Sample. The transparent TiO$_2$ film photoelectrodes were prepared by the procedure reported elsewhere.[17] The thickness of the TiO$_2$ thin films was about 4 μm measured with Alpha-Step 300 profiler (Tencor Instruments). The Ru−phenanthroline complexes were dissolved in dehydrated ethanol (Wako Chemicals) or a mixture solvent (50: 50) of *tert*-butyl alcohol (Kanto Chemicals) and acetonitrile (Kanto, dehydrated). These solvents were used without further purification. Detailed synthesis procedure of DCP2-TBA, DCP2, and MCPP has been reported elsewhere.[13−15] The semiconductor films were immersed into the dye solution at 25 °C to fix the dye onto the TiO$_2$ surface. The concentration of the adsorbate was monitored by absorption spectroscopy, and it was controlled by changing the immersion time in the dye solution. Typically, the absorbance of the sample specimen was around 0.5. The absorption spectra of dyes in ethanol and those of dyes adsorbed on the TiO$_2$ films were measured with an absorption spectrophotometer (Shimadzu, UV-3101PC).

Photocurrent Measurements. For the photocurrent measurements, a sandwich-type electrochemical cell consisting of a dye-adsorbed semiconductor electrode and a counter electrode separated by a spacer was used. The counter electrode was a Pt film sputtered on a SnO$_2$-coated glass (Nippon Sheet Glass Co.) using an ion coater (Eiko engineering, IB-5). These electrodes were immersed in an electrolyte solution consisting of 0.6 mol dm^{-3} 1,2-dimethyl-3-propylimidazolium iodide (DMPImI), 0.1 mol dm^{-3} LiI, 0.05 mol dm^{-3} I$_2$, and 0.5 mol dm^{-3} *tert*-butylpyridine (TBP) in methoxyacetonitrile. Reagent grade chemicals such as LiI (Wako Chemicals) and I$_2$ (Wako) were used as electrolytes. TBP (Aldrich) and methoxyacetonitrile (Tokyo Kasei) were distilled before measurements. DMPImI was synthesized from 1,2-dimethylimidazolium (Tokyo Kasei) and *n*-propyl iodide (Tokyo Kasei) according to the reported procedure.[40]

For the measurements of IPCE (incident photon to current conversion efficiency) of the solar cell, a 500 W halogen lamp combined with a monochromator (JASCO, CT-10) was used as a light source. Photocurrent was recorded with an ammeter (Keithley, model 2000) as a function of wavelength scanning with a wavelength controller (JASCO, SMD-25C). The light intensity of the monochromatic light was measured with an optical power meter (Advantest, TQ8210).

Transient Absorption Spectroscopy. For the transient absorption measurements, the second harmonic pulse (532 nm) from a Nd^{3+}:YAG laser (Continuum, Surelite II) was used for pumping. The duration of the laser pulse was 8 ns. A Xe flash
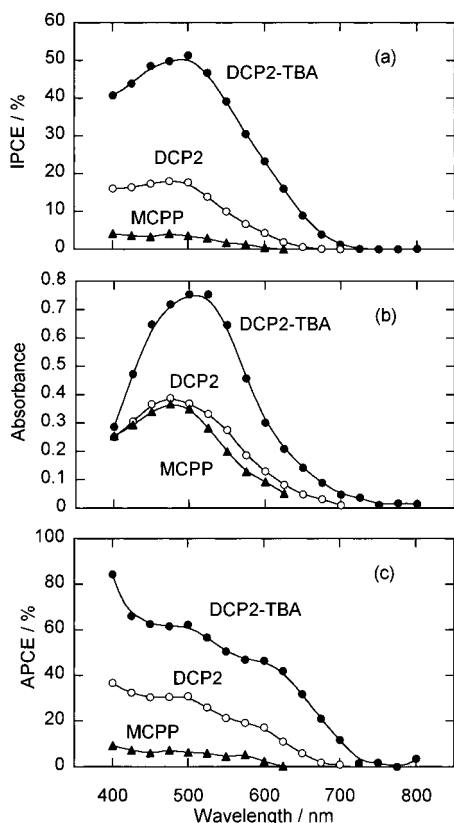
Figure 2. IPCE (a), absorption spectrum (b), and APCE (c) of the solar cells using the dyes indicated in Figure 1 as the sensitizer.

lamp (Hamamatsu, L4642, 2 μs pulse duration) was used as a probe light source. The probe light focused on a sample specimen (2 mm in diameter). The area irradiated by the probe light was covered with that by the exciting light (5 mm in diameter). All measurements were carried out under the same optical geometry to obtain the relative yields of transient species. The probe light transmitted through the sample specimen was detected with a Si photodiode (Hamamatsu, S-1722) after being dispersed with a monochromator (Ritsu, MC-10N). Signals from the photodetector were processed with a digital oscilloscope (Tektronix, TDS680C) and were analyzed with a computer. All measurements were carried out at room temperature.

Results and Discussion

Wavelength Dependence of Absorbed Photon-to-Current Conversion Efficiency (APCE). To study the mechanism of the solar cells, the incident photon-to-current conversion efficiency (IPCE) has been measured as a function of exciting wavelength.[39] The IPCE can be obtained as

$$\text{IPCE} = \frac{j_{\text{photo}}}{I_{\text{ex}}} \qquad (1)$$

where j_{photo} is the photocurrent and I_{ex} is the incident light intensity. Figure 2a shows the IPCEs of DCP2-TBA/TiO$_2$, DCP2/TiO$_2$, and MCPP/TiO$_2$ solar cells. Because the IPCE does not take into account the light harvesting efficiency of the solar cell, it is not well suited for detailed discussion of the photon-to-current conversion processes; IPCE has to be converted to the absorbed photon-to-current conversion efficiency (APCE). To evaluate APCE, IPCE is divided by the light harvesting
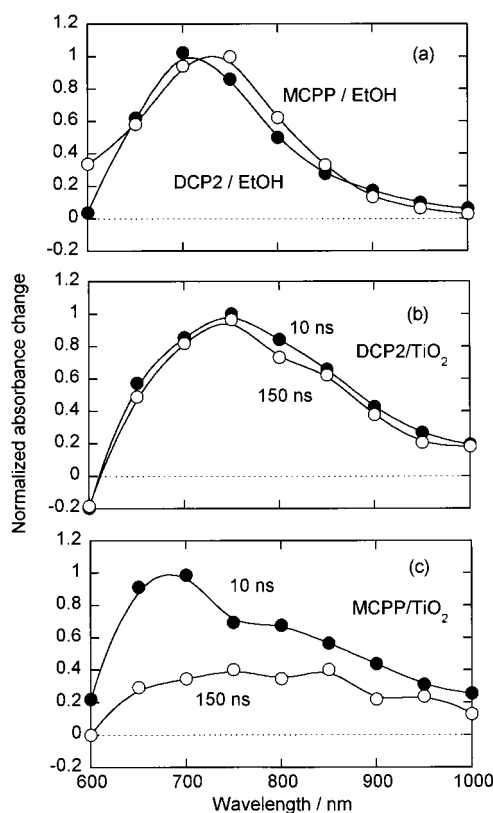

Figure 3. Transient absorption spectra obtained for DCP2 (filled circles) and MCPP (open circles) in ethanol (a), DCP2 on TiO$_2$ (b), and MCPP on TiO$_2$ (c) observed at 10 (filled circles) and 150 ns (open circles) after 532 nm light excitation.

efficiency

$$\text{APCE} = \frac{\text{IPCE}}{(1-T)} = \frac{\text{IPCE}}{(1 - 10^{-A})} \qquad (2)$$

where T is the transmittance and A is the absorbance of the exciting light. Using the absorption spectra shown in Figure 2b, the spectra of the APCE of DCP2-TBA/TiO$_2$, DCP2/TiO$_2$, and MCPP/TiO$_2$ solar cells are obtained (Figure 2c). The APCE of the DCP2/TiO$_2$ solar cell is about half of that of the DCP2-TBA/TiO$_2$ solar cell and about five times as large as that of the MCPP/TiO$_2$ solar cell. This clearly shows that the number of anchoring groups and the substitution of protons by TBAs affect the photon-to-current conversion efficiency.

Previously, we found that the solar-energy-to-electricity conversion efficiency of the MCPP/TiO$_2$ solar cell is considerably lower than that of the DCP2/TiO$_2$ solar cell.[14,15] We tentatively explained the low performance of the MCPP/TiO$_2$ solar cell as being due to the lower adsorption density of the dye on the TiO$_2$ film. The present results, however, show the lower photon-to-current conversion efficiency is responsible for the lower performance of the MCPP/TiO$_2$ solar cell.

Spectra and Decay Profiles of Transient Absorption. Figure 3a shows the transient absorption spectra of DCP2 and MCPP in ethanol just after excitation. The broad absorption band was observed for both DCP2 and MCPP with a maximum around 700 and 730 nm, respectively. The transient absorption of DCP2 and MCPP solutions decays with lifetimes of 20 and 50 ns, respectively. These lifetimes are similar to the luminescence lifetimes of the corresponding dyes in ethanol.[13,14] This indicates that the transient species observed are the dye molecules in the luminescent state, namely, the triplet metal-to-ligand charge transfer (^{3}MLCT) state.
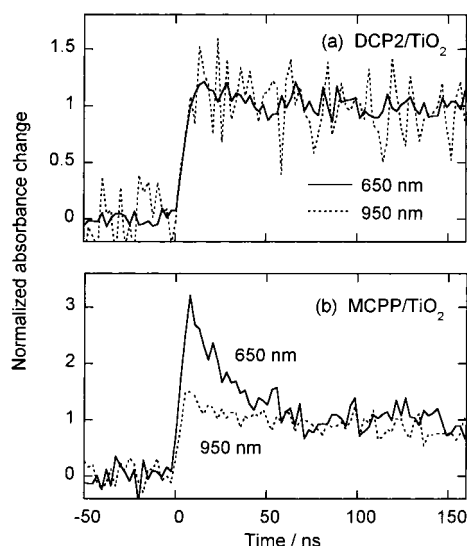
Nanocrystalline TiO$_2$ Films

J. Phys. Chem. B, Vol. 106, No. 2, 2002 **377**

Figure 4. Time profiles of the transient absorption obtained for DCP2/TiO$_2$ (a) and MCPP/TiO$_2$ (b) films at probe wavelengths of 650 (full line) and 950 nm (dashed line).

Figure 3 also shows the transient absorption spectra of dried films of DCP2/TiO$_2$ (b) and MCPP/TiO$_2$ (c) observed at 10 (filled circles) and 150 ns (open circles) after excitation. In DCP2/TiO$_2$, the broad absorption band was observed with a peak around 750 nm, and the spectrum does not change with time in this time range. The spectrum is different from that of the ^{3}MLCT in ethanol shown in Figure 3a, and the lifetime is considerably longer than that of the ^{3}MLCT (20 ns in ethanol). The spectrum observed is similar to the spectrum due to oxidized Ru(dcbpy)$_2$(NCS)$_2$ (N3) which has ligands similar to those of DCP2.[21,22] Therefore, the transient absorption spectrum observed for DCP2/TiO$_2$ can be assigned to that due to the oxidized DCP2. In contrast to DCP2/TiO$_2$, the transient absorption spectrum of MCPP/TiO$_2$ (Figure 3 c) changes with time. The spectrum at 10 ns has a peak around 700 nm, which is similar to that of ^{3}MLCT observed in solution (Figure 3 a). Therefore, the peak around 700 nm can be assigned to the absorption due to the ^{3}MLCT state. The spectrum at 150 ns has a peak around 800 nm, which is similar to that of DCP2/TiO$_2$ and, therefore, can be assigned to the absorption of the oxidized MCPP.

To study the formation and decay processes, we measured the time profile of the transient absorption of the dried films of DCP2-TBA/TiO$_2$, DCP2/TiO$_2$, and MCPP/TiO$_2$. It has been reported that the decay kinetics of transient absorption depends on the exciting light intensity under strong excitation condition.[32,34] The similar dependence was also observed in the present study. To eliminate the effect, the transient absorption measurements were carried out under low exciting light intensity (<0.4 mJ cm^{-1}). Figure 4 shows the time profiles of the transient absorption in DCP2/TiO$_2$ (a) and MCPP/TiO$_2$ (b) observed at 650 and 950 nm. The decay profiles are normalized at 150 ns. DCP2-TBA/TiO$_2$ shows decay profiles similar to those of DCP2/TiO$_2$. The time profile observed at 650 nm mainly shows generation and decay processes of the ^{3}MLCT state, and a small contribution of the oxidized dye is expected. The time profile observed at 950 nm should show the generation and decay processes of the oxidized dye, because the absorption due to ^{3}MLCT state has only a small contribution at 950 nm as shown in Figure 3a.

As shown in Figure 4a, the oxidized DCP2 on TiO$_2$ film is produced within the time resolution of the instrument, and the absorption due to ^{3}MLCT does not appear at short times. This indicates that the electron injection occurs much faster than the lifetime of the ^{3}MLCT state; namely, the efficiency of the electron injection of DCP2/TiO$_2$ is very high.

The formation of the oxidized MCPP seems to occur within the time resolution of the instrument as seen from the curve of 950 nm in Figure 4b. This shows that the electron injection occurs very fast from the excited state. However, ^{3}MLCT still exists on the film after the fast electron injection (the 650 nm curve in Figure 4b). This indicates that some fraction of MCPP dyes undergoes very fast electron injection, whereas the remainder part does not. This can be considered as being due to the existence of two adsorption sites in MCPP/TiO$_2$: for *active dye*, which is effective for electron injection, and for *inactive dye*, which is not effective for electron injection.

The fast component of the transient absorption at 650 nm assigned to the ^{3}MLCT state (Figure 4b) can be fitted with a 20 ns lifetime. This is shorter than the lifetime of ^{3}MLCT in ethanol (50 ns). The quenching may be due to nonradiative decay channels induced at the surface. The quenching by electron injection can be ruled out because no corresponding rise-up of the absorption of the oxidized MCPP was observed as shown in Figure 4b.

Relative Efficiency of Electron Injection. Electronic excitation of a dye molecule adsorbed on TiO$_2$ leads to the formation of an injected electron and an oxidized dye. As shown in Figure 3 parts b and c, the absorbance change due to the oxidized molecules can be measured, and therefore, the injection efficiency can be estimated. At present, however, the molar absorption coefficients of the oxidized DCP2 and oxidized MCPP are not known. Thus, we cannot estimate the absolute number of oxidized dyes from the transient absorption spectra observed.

As shown in Figure 3 parts b and c, the absorption spectra of the oxidized DCP2 and oxidized MCPP on TiO$_2$ are similar. Thus, we assume that the molar absorption coefficients of these oxidized dyes are equal. From the absorbance change A_{ox} of the oxidized dye and the number N_{photon} of absorbed photons, the relative injection efficiency Φ_{inj}^{rel} can be expressed as

$$\Phi_{inj}^{rel} = \frac{A_{OX}}{N_{photon}} \qquad (3)$$

As shown in Figure 4b, the absorbance change of the ^{3}MLCT state decays with time in an earlier time range in MCPP/TiO$_2$ and it becomes constant at 150 ns. On the contrary, the absorbance change of the oxidized dye observed at 950 nm does not decay in this time range. Therefore, we can take the absorbance change at 150 ns after excitation as A_{ox}.

Figure 5 shows the absorbance change observed at 825 nm at 150 ns of DCP2-TBA/TiO$_2$, DCP2/TiO$_2$, and MCPP/ TiO$_2$ as a function of the number N_{photon} of absorbed photons. N_{photon} is evaluated as a product of the exciting light intensity I_{ex} and the light harvesting efficiency, $1 - T$, where T is the transmittance of the sample film at the excitation wavelength (532 nm). We measured the transient absorption at various exciting light intensities (0.02−0.36 mJ cm^{-2}) and for sample specimens having different amount of adsorbed dyes (absorbance at 532 nm: 0.3−0.5). As seen from Figure 5, A_{ox} is proportional to the number of absorbed photons. The slope of the line gives the relative efficiency of electron injection (see eq 3). The electron injection efficiency of DCP2/TiO$_2$ is almost equal to that of DCP2-TBA/TiO$_2$ and approximately four times as large as that of MCPP/TiO$_2$. If we assume an appropriate value for the molar absorption coefficient of the oxidized dyes at 825 nm, the absolute efficiency of electron injection can be estimated. Using a value of 5000 mol^{-1} dm^3 cm^{-1} as the molar
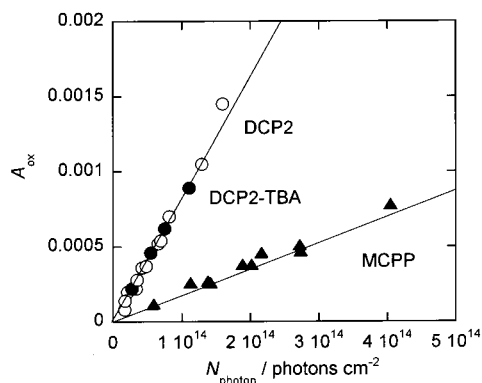
Figure 5. Absorbance change probed at 825 nm at 150 ns after excitation as a function of the number of absorbed photons for DCP2-TBA/TiO$_2$ (filled circles), DCP2/TiO$_2$ (open circles), and MCPP/TIO$_2$ (filled triangles).

absorption coefficient, the absolute efficiency of electron injection can be estimated as $\Phi_{inj} = 0.6$.

As we mentioned above, for MCPP/TiO$_2$, the fast decay component observed at 650 nm in Figure 4b (20 ns lifetime) is due to the ^{3}MLCT state of the inactive dye, which is not effective for electron injection, and the slow component is due to the oxidized state produced from the active dye. The abundance of the inactive dye on the surface can be evaluated by comparing the absorbance of the ^{3}MLCT state with that of the oxidized state. For N3/TiO$_2$, the molar absorption coefficient of the oxidized N3 at 650 nm is similar in magnitude to that of the ^{3}MLCT state at the same wavelength.[21,22] From the similarity of the electronic state between N3 and MCPP, we assume that the molar absorption coefficient of the oxidized MCPP at 650 nm is equal to that of the ^{3}MLCT state at the same wavelength. As shown in Figure 4b, after the fast decay which is assigned to ^{3}MLCT state about 30% of the initial value of the absorbance remains. This shows that 70% of MCPP molecules on TiO$_2$ acts as the inactive dyes. Roughly speaking, this is parallel to the difference between the relative electron injection efficiencies of DCP2/TiO$_2$ and MCPP/TiO$_2$ as shown in Figure 5, and therefore, the low injection efficiency of MCPP/TiO$_2$ can be considered to be due to the existence of inactive dyes. For DCP2-TBA/TiO$_2$ and DCP2/TiO$_2$, inactive dyes are not observed. This suggests that the efficiency of electron injection in DCP2-TBA/TiO$_2$ and DCP2/TiO$_2$ is very high.

We conclude that the low efficiency of the electron injection in MCPP/TiO$_2$ is due to the presence of the inactive dye on the surface. Although there is no detailed information about the inactive dyes, we discuss some possibilities of the origin of the inactive dyes observed in MCPP/TiO$_2$. One possibility is the aggregate of the sensitizer molecules. It has been reported that IPCE is reduced by aggregation of the sensitizer molecules.[41] This may be due to the low efficiency of the electron injection from the aggregate; namely, the aggregate is the inactive dyes. In the preparation of the sample specimen of MCPP/TiO$_2$, we put small amount of dyes on the surface as seen from the absorbance in Figure 2b. Thus, the presence of the aggregate on the surface can be ruled out. Moreover, the absorption spectrum of MCPP/TiO$_2$ is similar to that of MCPP in solution, suggesting no aggregation on the surface.

The presence of two ^{3}MLCT excited states in MCPP may also be the possible origin of the inactive dyes. MCPP has two kinds of phenanthroline ligands. One is the ligand with a carboxyl group attached directly to the TiO$_2$ surface (adjacent ligand) and the other is the ligand without a carboxyl group (remote ligand). The electron injection from both adjacent and

remote ligand excited states is energetically possible. In fact, the electron injection from a remote ligand excited state has been reported.[42] The remote ligand injection can be considered to be inefficient because the electronic coupling with the TiO$_2$ surface is small. Accordingly, if the excitation energy hopping rate between the adjacent and remote ligands is much slower than the lifetime of the excited state, we may observe the electron injection from the adjacent ligand and the emission from the remote ligand. In fact, however, it has been found that MCPP in solution shows emission from only one excited state.[13] This indicates that the excited state is not localized at one of the ligands; namely, excitation energy hopping between the ligands is very fast. From the results of cyclic voltammetries of the complexes, it has been found that the energy level of the ^{3}MLCT state of the remote ligand is lower than that of the adjacent ligand.[14] Accordingly, we consider that the excited state is localized on the adjacent ligand after excitation energy hopping. Thus, we consider that the inefficient electron injection from the remote ligand excited state is unlikely for the origin of the inactive dyes, and the electron injection may occur through the adjacent ligand after excitation energy hopping.

It has been reported that fast electron injection processes (<100 fs to 10 ps) have been reported for many sensitizing dyes having carboxyl groups as anchors.[21-30] Accordingly, it is expected that the electron injection from the MCPP molecule adsorbed through the carboxyl group is fast and efficient. Thus, we consider that the inactive dyes are not adsorbed on TiO$_2$ through the carboxyl group. It has been found that strong binding to the TiO$_2$ surface through the carboxyl group occurs in many Ru−complexes. For MCPP/TiO$_2$, we can consider that adsorption to TiO$_2$ surface is not so strong, because the absorbance of MCPP/TiO$_2$ specimen is much smaller than that of DCP2 and N3 on the same specimen under the same immersion period in dye solution. Accordingly, the adsorption of MCPP to the TiO$_2$ surface by another adsorption mode may be possible. It has been reported that Fe(CN)$_6$$^{4-}$ and Fe(bipyridine)(CN)$_4$$^{2-}$ are adsorbed on TiO$_2$ through the CN groups.[43-45] Both CN and NCS groups are electron-withdrawing groups, and therefore, MCPP is considered to be adsorbed on TiO$_2$ through the NCS groups. It is known that the rate of electron transfer reaction rapidly decreases with increasing distance between the donor and the acceptor. In the excited state of MCPP, the electron in LUMO is localized at the phenanthroline ligand. In the conformation of MCPP adsorbed through the carboxyl group, the ligand is located near the TiO$_2$ surface, so that efficient injection can be realized. On the contrary, in the conformation of MCPP adsorbed through the NCS groups, the ligand is far apart from the TiO$_2$ surface. Accordingly, the electron injection efficiency is expected to be low.

Relation between the Relative Injection Efficiency and APCE. We shall compare the APCE of the solar cell with the relative electron injection efficiency obtained for the dried films by the transient absorption spectroscopy. As shown in Figure 5, the injection efficiency of DCP2/TiO$_2$ is four times as large as that of MCPP/TiO$_2$. This difference is similar to that in the APCE between the DCP2/TiO$_2$ and MCPP/TiO$_2$ solar cells shown in Figure 2c. This clearly shows that the difference in the APCE between the DCP2/TiO$_2$ and MCPP/TiO$_2$ solar cells is due to the difference in the electron injection efficiency.

The absolute values of the APCE of the DCP2/TiO$_2$ solar cell shown in Figure 2c is 30% at 500 nm; namely, 70% of photons absorbed are not converted to conducting electrons in the external circuit. This relatively low APCE was improved to 60% by substitution of protons by TBAs as shown in Figure 2c. As it is well-known that the energy level of the conduction

Nanocrystalline TiO$_2$ Films

J. Phys. Chem. B, Vol. 106, No. 2, 2002 **379**

band edge is reduced by adsorption of protons to the TiO$_2$ surface, the rate of the electron injection may be affected by the substitution. In reality, however, the efficiency of the electron injection is not affected by the substitution as shown in Figure 5. This indicates that the electron injection for both DCP2/TiO$_2$ and DCP2-TBA/TiO$_2$ occurs much faster than the deexcitaiton of the excited state. As shown in Figure 4, the absorption change due to the oxidized dyes does not decay in this time range. This indicates that the recombination rate is slower than the rereduction rate of the oxidized dye by the iodide redox mediator, which was reported to occur in 0.1−1 μs.[33−35] Therefore, it is considered that the recombination process is not the major loss channel of the injected electrons in the solar cell. Accordingly, the low APCE of the DCP2/TiO$_2$ solar cell compared with that of DCP2-TBA/TiO$_2$ is due to the more efficient reaction of conducting electrons with the redox mediator (dark current). The APCE (60%) for DCP2-TBA/TiO$_2$ is higher than that of DCP2/TiO$_2$ (30%), whereas the electron injection efficiency is almost equal. This implies that the substitution of the protons by TBAs reduced the efficiency of the dark current (process 4). The reason may be that the approach of the redox mediators to the TiO$_2$ surface is hindered by the presence of bulky TBAs on the surface.

Conclusion

We have measured the electron injection efficiency of Ru−phenanthroline complexes adsorbed on TiO$_2$ nanocrystalline films and compared it with the APCE of the solar cells. We found that the electron injection efficiency of DCP2/TiO$_2$ (four carboxyl groups) is four times as large as that of MCPP/ TiO$_2$ (one carboxyl group). From the decay profile of the transient absorption, we conclude that the lower efficiency of MCPP/ TiO$_2$ is due to the presence of the inactive dye on the TiO$_2$ surface, which is not effective for electron injection. We also studied the effect of the countercations of DCP2 by substituting the two protons of the ligand by two tetrabutylammonium (TBA) ions. The APCE of the solar cell using the dye with substituted ligands (DCP2-TBA) is higher than that of DCP2, although the relative injection efficiency is similar. This implies that TBA inhibits the reaction of conducting electrons in TiO$_2$ with I$^-$/I$_3^-$ redox mediators. These results show that the photon-to-current conversion process of the solar cell is sensitive to the ligand structure of the sensitizing dye. Accordingly, we have to design the ligand structure of the sensitizing dye carefully in order to develop high-performance solar cells.

References and Notes

(1) Nazeeruddin, M. K.; Kay, A.; Rodicio, I.; Humphry-Baker, R.; Muller, E.; Liska, P.; Vlachopoulos, N.; Grätzel, M. *J. Am. Chem. Soc.* **1993**, *115*, 6382−6390.

(2) Argazzi, R.; Bignozzi, C. A.; Heimer, T. A.; Castellano, F. N.; Meyer, G. J. *J. Inorg. Chem.* **1994**, *33*, 5741−5749.

(3) Nazeeruddin, Md. K.; Pèchy, P.; Grätzel, M. *J. Chem. Soc., Chem. Commun.* **1997**, 1705−1706.

(4) Argazzi, R.; Bignozzi, C. A.; Hasselmann, G. M.; Meyer, G. J. *Inorg. Chem.* **1998**, *37*, 4533−4537.

(5) Zakeeruddin, S. M.; Nazeeruddin, Md. K.; Humphry-Baker, R.; Grätzel, M. *Inorg. Chem.* **1998**, *37*, 5251−5259.

(6) Aranyos, V.; Grennberg, H.; Tingry, S.; Lindquist, S.-E.; Hagfeldt, A. *Sol. Energy Mater. Sol. Cells* **2000**, *64*, 97−114.

(7) Nazeeruddin, Md. K.; Pèchy, P.; Renouard, T.; Zakeeruddin, S. M.; Humphry-Baker, R.; Comte, P.; Liska, P.; Cevey, L.; Costa, E.; Shklover, V.; Spiccia, L.; Deacon, G. B.; Bignozzi, C. A.; Grätzel, M. *J. Am. Chem. Soc.* **2001**, *123*, 1613−1624.

(8) Sauvé, G.; Cass, M. E.; Coia, G.; Doig, S. J.; Lauermann, I.; Pomykal, K. E.; Lewis, N. S. *J. Phys. Chem. B*. **2000**, 104, 6821−6836.

(9) Wang, Z.-S.; Li, F.-Y.; Huang, C.-H.; Wang, L.; Wei, M.; Jin, L.-P.; Li, N. Q. *J. Phys. Chem.* **2000**, *104*, 9676−9682.

(10) Islam, A.; Hara, K.; Singh, L. P.; Katoh, R.; Yanagida, M.; Murata, S.; Takahashi, Y.; Sugihara, H.; Arakawa, H. *Chem. Lett.* **2000**, 490−491.

(11) Sugihara, H.; Singh, L. P.; Sayama, K.; Arakawa, H.; Nazeeruddin, Md. K.; Grätzel, M. *Chem. Lett.* **1998**, 1005−1006.

(12) Takahashi, Y.; Arakawa, H.; Sugihara, H.; Hara, K.; Islam, A.; Katoh, R.; Tachibana, Y.; Yanagida, M. *Inorg. Chim. Acta* **2000**, *310*, 169−174.

(13) Yanagida, M.; Singh, L. P.; Sayama, K.; Hara, K.; Katoh, R.; Islam, A.; Sugihara, H.; Arakawa, H.; Nazeerddin, Md. K.; Grätzel, M. *J. Chem. Soc., Dalton Trans.* **2000**, 2817−2822.

(14) Hara, K.; Sugihara, H.; Singh, L. P.; Islam, A.; Katoh, R.; Yanagida, M.; Sayama, K.; Murata, S.; Arakawa, H. *J. Photochem. Photobiol. A: Chem.* **2001**, *145*, 117−122.

(15) Hara, K.; Sugihara, H.; Tachibana, Y.; Islam, A.; Yanagida, M.; Sayama, K.; Arakawa, H.; Fujihashi, G.; Horiguchi, T.; Kinoshita, T. *Langmuir* **2001**, *17*, 5992−5999.

(16) Islam, A.; Sugihara, H.; Hara, K.; Singh, L. P.; Katoh, R.; Yanagida, M.; Takahashi, Y.; Murata, S.; Arakawa, H. *New J. Chem.* **2000**, *24*, 343−345.

(17) Hara, K.; Horiguchi, T.; Kinoshita, T.; Sayama, K.; Sugihara, H.; Arakawa, H. *Sol. Energy Mater. Sol. Cells* **2000**, *64*, 115−134.

(18) Sayama, K.; Hara, K.; Mori, N.; Satsuki, M.; Suga, S.; Tsukagoshi, S.; Abe, Y.; Sugihara, H.; Arakawa, H. *Chem. Commun.* **2000**, 1173−1174.

(19) Sayama, K.; Hara, K.; Ohga, Y.; Shinpo, A.; Suga, S.; Arakawa, H. *New. J. Chem.* **2001**, *25*, 200−202.

(20) Hara, K.; Sayama, K.; Ohga, Y.; Shinpo, A.; Suga, S.; Arakawa, H. *Chem. Commun.* **2001**, 569−570.

(21) Tachibana, Y.; Moser, J. E.; Grätzel, M.; Klug, D. R.; Durrant, J. R. *J. Phys. Chem.* **1996**, *100*, 20056−20062.

(22) Tachibana, Y.; Haque, S. A.; Mercer, I. P.; Durrant, J. R.; Klug, D. R. *J. Phys. Chem. B* **2000**, *104*, 1198−1205.

(23) Hannappel, T.; Burfeindt, B.; Storck, W.; Willig, F. *J. Phys. Chem. B* **1997**, *101*, 6799−6802.

(24) Asbury, J. B.; Ellingson, R. J.; Ghosh, H. N.; Ferrere, S.; Nozik, A. J.; Lian, T. *J. Phys. Chem. B* **1999**, *103*, 3110−3119.

(25) Asbury, J. B.; Hao, E.; Wang, Y.; Ghosh, H. N.; Lian, T. *J. Phys. Chem. B* **2001**, *105*, 4545−4557.

(26) Bauer, C.; Boschloo, G.; Mukhtar, E.; Hagfeldt, A. *J. Phys. Chem. B* **2001**, *105*, 5585−5588.

(27) Asbury, J. B.; Hao, E.; Wang, Y.; Lian, T. *J. Phys. Chem. B* **2000**, *104*, 11957−11957.

(28) Iwai, S.; Hara, K.; Murata, S.; Katoh, R.; Sugihara, H.; Arakawa, H. *J. Chem. Phys.* **2000**, *113*, 3366−3373.

(29) Kamat, P. V.; Bedja, I.; Hotchandani, S.; Patterson, L. K. *J. Phys. Chem.* **1996**, *100*, 4900−4908.

(30) Benkö, G.; Hilgendorff, M.; Yartsev, A. P.; Sundström, V. *J. Phys. Chem. B* **2001**, *105*, 967−974.

(31) O'Regan, B.; Moser, J.; Anderson, M.; Grätzel, M. *J. Phys. Chem.* **1990**, *94*, 8720−8726.

(32) Haque, S. A.; Tachibana, Y.; Willis, R. L.; Moser, J. E.; Grätzel, M.; Klug, D. R.; Durrant, J. R. *J. Phys. Chem. B* **2000**, *104*, 538−547.

(33) Heimer, T. A.; Heilweil, E. J.; Bignozzi, C. A.; Meyer, G. J. *J. Phys. Chem. A* **2000**, *104*, 4256−4262.

(34) Haque, S. A.; Tachibana, Y.; Klug, D. R.; Durrant, J. R. *J. Phys. Chem. B* **1998**, *102*, 1745−1749.

(35) Kuciauskas, D.; Freund, M. S.; Gray, H. B.; Winkler, J. R.; Lewis, N. S. *J. Phys. Chem. B* **2001**, *105*, 392−403.

(36) Solbrand, A.; Lindström, H.; Rensmo, H.; Hagfeldt, A.; Lindquist, S.; Södergren, S. *J. Phys. Chem. B* **1997**, *101*, 2514−2518.

(37) Duffy, N. W.; Peter, L. M.; Rajapakse, R. M. G.; Wijayantha, K. G. U. *J. Phys. Chem. B* **2000**, *104*, 8916−8919.

(38) Kalyanasundaram, K.; Grätzel, M. *Coord. Chem. Rev.* **1998**, 77, 347−414.

(39) Hagfeldt, A.; Grätzel, M. *Chem. Rev.* **1995**, 95, 49−68.

(40) Bonhôte, P.; Dias, A. P.; Papageorgiou, N.; Kalyanasundram, K.; Grätzel, M. *Inorg. Chem.* **1996**, *35*, 1168−1178.

(41) Khazraji, A. C.; Hotchandani, S.; Das, S.; Kamat, P. V. *J. Phys. Chem. B* **1999**, *103*, 4693−4700.

(42) Qu, P.; Thompson, D. W.; Meyer, G. J. *Langmuir* **2000**, *16*, 4662−4671.

(43) Vrachnou, E.; Vlachopoulos, N.; Grätzel, M. *J. Chem. Soc., Chem. Commun.* **1987**, 868−874.

(44) Vrachnou, E.; Grätzel, M.; McEvoy, A. *J. Electroanal. Chem.* **1989**, *258*, 193−197.

(45) Yang, M.; Thompson, D. W.; Meyer, G. J. *Inorg. Chem.* **2000**, *39*, 3738.